



저작자표시-비영리-변경금지 2.0 대한민국

이용자는 아래의 조건을 따르는 경우에 한하여 자유롭게

- 이 저작물을 복제, 배포, 전송, 전시, 공연 및 방송할 수 있습니다.

다음과 같은 조건을 따라야 합니다:



저작자표시. 귀하는 원저작자를 표시하여야 합니다.



비영리. 귀하는 이 저작물을 영리 목적으로 이용할 수 없습니다.



변경금지. 귀하는 이 저작물을 개작, 변형 또는 가공할 수 없습니다.

- 귀하는, 이 저작물의 재이용이나 배포의 경우, 이 저작물에 적용된 이용허락조건을 명확하게 나타내어야 합니다.
- 저작권자로부터 별도의 허가를 받으면 이러한 조건들은 적용되지 않습니다.

저작권법에 따른 이용자의 권리는 위의 내용에 의하여 영향을 받지 않습니다.

이것은 [이용허락규약\(Legal Code\)](#)을 이해하기 쉽게 요약한 것입니다.

[Disclaimer](#)

의학박사 학위논문

Oncologic safety and efficacy of  
cell-assisted lipotransfer for  
breast reconstruction in a murine  
model of residual breast cancer

유방암 잔여 동물모델에서 유방재건을 위한 세포 보조  
지방이식의 종양학적 안전성 및 유효성

2023년 2월

서울대학교 대학원  
의학과 성형외과학 전공

JIN XIAN

유방암 잔여 동물모델에서 유방재  
건을 위한 세포 보조 지방이식의  
종양학적 안전성 및 유효성

지도 교수 장학

이 논문을 의학박사 학위논문으로 제출함  
2022년 10월

서울대학교 대학원  
의학과 성형외과학 전공  
JIN XIAN

JIN XIAN의 의학박사 학위논문을 인준함  
2023년 1월

위원장 \_\_\_\_\_ (인)

부위원장 \_\_\_\_\_ (인)

위원 \_\_\_\_\_ (인)

위원 \_\_\_\_\_ (인)

위원 \_\_\_\_\_ (인)

# Oncologic safety and efficacy of cell-assisted lipotransfer for breast reconstruction in a murine model of residual breast cancer

A thesis submitted to the Department of Plastic and Reconstructive Surgery in fulfillment of the requirements for the Degree of Doctor of Philosophy in Medicine at Seoul National University College of Medicine

October 2022

Graduate School of College of Medicine  
Seoul National University  
Department of Plastic and Reconstructive Surgery Major  
JIN XIAN

Confirming the Ph.D. Dissertation written by  
JIN XIAN  
January 2023

Chair	_____	(Seal)
Vice Chair	_____	(Seal)
Examiner	_____	(Seal)
Examiner	_____	(Seal)
Examiner	_____	(Seal)

# Abstract

## Oncologic safety and efficacy of cell–assisted lipotransfer for breast reconstruction in a murine model of residual breast cancer

XIAN JIN

College of Medicine

Department of Plastic and Reconstructive Surgery

The Graduate School

Seoul National University

**Background:** Cell–assisted lipotransfer (CAL) is a novel technique for fat grafting that combines the grafting of autologous fat and adipose–derived stromal cells (ASCs) to enhance fat graft retention; however, its oncologic safety is controversial.

**Methods:** Herein, we investigated the oncologic safety of CAL for breast reconstruction using a murine model of residual breast cancer. Various concentrations of 4T1 cells (murine breast cancer cells) were injected into female mastectomized BALB/c mice to determine the appropriate concentration for injection. One week after injection, mice were divided into control (100  $\mu$ L fat), low CAL ( $2.5 \times 10^5$  ASCs/100  $\mu$ L fat), and high CAL ( $1.0 \times 10^6$  ASCs/100  $\mu$ L fat) groups, and fat grafting was performed. The injection of  $5.0 \times 10^3$  4T1 cells was appropriate to produce a murine model of residual breast cancer.

**Results:** The weight of the fat tumor mass was significantly higher in the high CAL group than in the other groups ( $p < 0.05$ ). However,

the estimated tumor weight was not significantly different between the groups. Additionally, the fat graft survival rate was significantly higher in the high CAL group than in the control and low CAL groups ( $p < 0.05$ ). No significant difference was noted in the percentage of Ki-67-positive cells, suggesting that tumor proliferation was not significantly different between the groups.

**Conclusion:** In summary, CAL significantly improved fat graft survival without affecting tumor size and proliferation in a murine model of residual breast cancer. These results highlight the oncologic safety of CAL for breast reconstruction.

---

Keywords: Adipose-derived stromal cells; cell-assisted lipotransfer; fat graft; murine breast cancer model

Student Number: 2020-36902

# Table of Contents

Abstract .....	i
Table of Contents .....	iii
List of Tables .....	iv
List of Figures .....	iv
<b>1. Introduction .....</b>	<b>1</b>
1.1. Study Background .....	1
1.2. Purpose of Research .....	3
<b>2.1. Material and methods .....</b>	<b>4</b>
2.1.1 Cell culture .....	4
2.1.2 Orthotopic mouse model of residual breast cancer .....	4
2.1.3 Histomorphometric evaluation .....	6
2.1.4 Gene expression analysis .....	8
2.1.5 Statistical analysis .....	8
<b>2.2. Results .....</b>	<b>9</b>
2.2.1 Determining the optimal concentration of 4T1 cells to produce an orthotopic residual breast cancer model .....	9
2.2.2 Quantitative and qualitative analysis of the grafted fat and tumor mass .....	10
2.2.3 CAL enhance grafted fat survival and facilitate the revascularization in grafted fat .....	13
2.2.4 Gene expression analysis .....	15
<b>2.3. Discussion .....</b>	<b>18</b>
<b>3. Conclusion .....</b>	<b>22</b>
<b>Bibliography .....</b>	<b>23</b>
<b>Figure Legends .....</b>	<b>31</b>
<b>Abstract in Korean .....</b>	<b>35</b>

## List of Table

Table 1. Primer sequences for quantitative real-time polymerase chain reaction .....	30
--	----

## List of Figures

Figure 1. Schematic illustrate of the cell-assisted lipotransfer .....	3
Figure 2. Schematic overview of the animal study design ....	5
Figure 3. Experiment group of baseline, control, low CAL, and high CAL groups.....	6
Figure 4. Bioluminescent imaging for determining the optimal number of cancer cells for injection.....	9
Figure 5. Gross observation and measurement of tumor mass four weeks after injection of 4T1 cells and three weeks after fat/CAL graft.....	10
Figure 6. Gross examination of the tumor in the experimental groups. ..	11
Figure 7. Representative hematoxylin and eosin-stained sections of the fat tumor mass from each group. Measurement of the Ki-67 proliferative index. ....	12
Figure 8. Immunostaining of vessel distribution in grafted fat.....	14
Figure 9. Whole-mount immunostaining of three experimental group grafted fat.....	15
Figure 10. Expression of different genes from grafted fat and tumor.....	17
Figure 11. Schematic diagram of animal experiments. ....	19
Figure Legends .....	31



# 1. Introduction

## 1.1. Study Background

Autologous fat grafts have been accepted as a suitable reconstructive method for small breast defects. In recent years, the number of patients undergoing breast-conserving surgeries has increased, and thus, the demand for breast reconstruction with fat grafts has also increased [1]. Compared with autologous flap reconstruction, autologous fat graft presents advantages including minimal damage to the donor site and an easily available source of fat for performing multiple revisions of breast reconstruction, especially with partial breast reconstruction. However, the main drawback of conventional autologous fat grafting is that it is associated with an average 50% volume loss of the graft [2–5].

Attempts have been made to use stromal vascular fraction (SVF)-based cell-assisted lipotransfer (CAL) for adjunct breast reconstruction to reduce graft loss (Fig. 1). CAL is a fat grafting technique in which isolated SVFs are supplemented to increase the concentration of adipose-derived stromal cells (ASCs). Both *in vitro* and *in vivo* studies have suggested that ASC-based CAL could improve the survival of fat grafts in breast augmentation and facial lipotransfer [6, 7]. In a randomized controlled clinical study, ASC-enriched fat grafts had significantly higher survival rates (mean = 80.2%) than conventional fat grafts (mean = 45.1%) in breast reconstruction [8]. These results suggest that ASC-based CAL is an attractive alternative to conventional fat grafting owing to higher fat volume retention.

Some evidence suggests that ASCs increase cancer cell

proliferation and migration [9]. Additionally, in vitro studies have reported that ASCs might influence cancer cell proliferation through cytokines, chemokines, and cell-to-cell paracrine signaling [10,11]. Although the efficacy of CAL in breast reconstruction has been reported, there is a persistent debate about the oncological risks associated with autologous fat grafting combined with cell enrichment.

However, there are also conflicting reports that fat grafting and CAL do not affect, or in fact suppress, cancer cell proliferation owing to pro-apoptotic characteristics, as well as through the production of anti-proliferative chemokines [12]. In vitro studies using human ASCs and various human breast cell lines have reported that the transplantation of ASCs is unlikely to increase tumor recurrence [10,13–15]. In a recent in vivo study in which nude mice were sequentially injected with different human breast cancer cell lines and adipose tissue, fat graft was not associated with an increase in tumor recurrence [16]. A large-scale case-control clinical study of 633 patients undergoing breast reconstruction concluded that there was no difference in oncologic risk between the ASC-enriched fat graft and control groups [17]. Similarly, an increased incidence of cancer recurrence was not observed in a long-term follow-up study examining SVF-enriched fat grafts after breast cancer surgery [18]. Additionally, there is no evidence that suggests the malignant conversion of cultured human mesenchymal stem cells (MSCs) or ASCs [19].

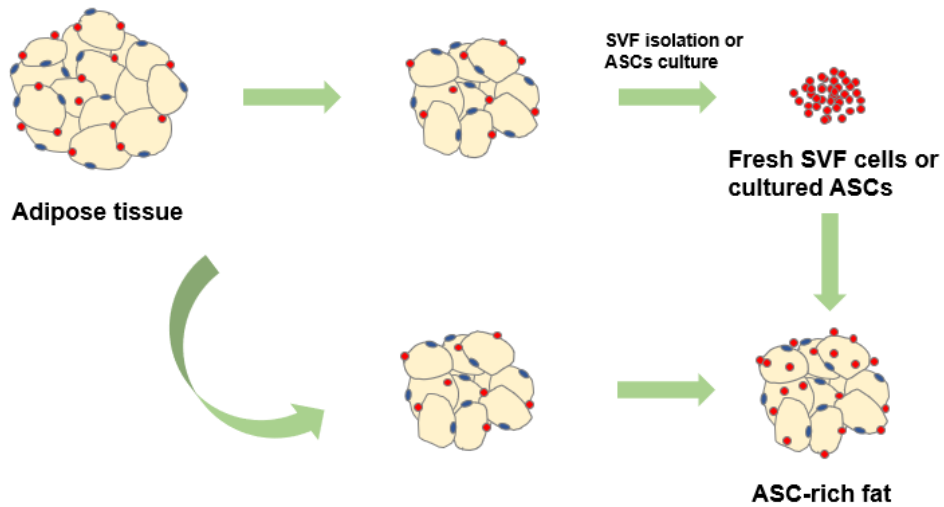


Figure 1. Schematic illustrate of the cell-assisted lipotransfer (CAL).

## 1.2. Purpose of Research

Although a few clinical studies on CAL have been published, there is a lack of standard protocols for ASC- or SVF-based cell therapy. Additionally, studies have not clarified the safety of ASC-containing CAL, and few studies have reported on the efficacy and safety of these approaches. Therefore, in the present study, we examined the efficacy and safety of CAL with different concentrations of ASCs using a suitable animal model. As patients with breast cancer are the most common candidates who undergo CAL for breast reconstruction in clinical practice, we used a murine model of breast cancer. There was difficulty in preparing an ideal animal model as a breast cancer recurrence model. Experiments were conducted with the cancer residual model. The aim of the present study was to identify optimal treatment conditions for CAL to improve fat graft survival outcomes and to evaluate its oncological safety.

## 2.1. Material and methods

### 2.1.1 Cell culture

For the primary culture of ASCs, inguinal adipose tissue was harvested from a 7-week-old female BALB/C donor mouse. The harvested adipose tissue was digested with 0.2% collagenase type I (Worthington Biochemical Corp., Lakewood, NJ) at 37 ° C for 1 h and centrifuged at 1500 rpm for 3 min [20]. The cell pellet was resuspended in Dulbecco ' s modified Eagle ' s medium (DMEM)/F12+GlutaMAX™ supplemented with 10% fetal bovine serum (FBS; both from Invitrogen, Waltham, MA) and 1% penicillin–streptomycin (Gibco, Waltham, MA) and maintained at 37 ° C in a 5% CO2 incubator.

The murine breast cancer cell line 4T1 and green fluorescent protein (GFP)–expressing 4T1 cells were donated. The cells were cultured in RPMI–1640 media (HyClone, Logan, UT) supplemented with 10% FBS (Invitrogen) and 1% penicillin–streptomycin (Gibco) and were maintained at 37 ° C in a 5% CO2 incubator.

### 2.1.2 Orthotopic mouse model of residual breast cancer

We used a modified version of a previously described orthotopic breast cancer animal model [21]. Seven-week-old female BALB/c mice (Orient Co., Seoul, Korea) were allowed to acclimatize for 1 week before use in experiments. All experiments involving animals were approved by the Institutional Animal Care and Use Committee (IACUC) of Seoul National University Hospital (IACUC No.20–0083–S1A1). All experiments were performed in accordance with

relevant guidelines and regulations, including ARRIVE. The animals were provided with food and water ad libitum. First, we performed an in vivo imaging study to determine the optimal cell number to establish a murine model of residual breast cancer. Next, mice were injected with different concentrations of GFP-expressing 4T1 cells ( $1.0 \times 10^3$ ,  $5.0 \times 10^3$ , and  $1.0 \times 10^4$ ) in the third mammary fat pad and examined 4 weeks after injection. The IVIS Lumina II Imaging System (PerkinElmer, Waltham, MA) was used to detect in situ fluorescent signals from Green CMFDA Dye as per the manufacturer's instructions. Anesthetized mice were imaged using a 20 cm field of view and an exposure time of 1 s. The excitation and emission filters for the Green CMFDA Dye signal were set from 480 to 520 nm [22].

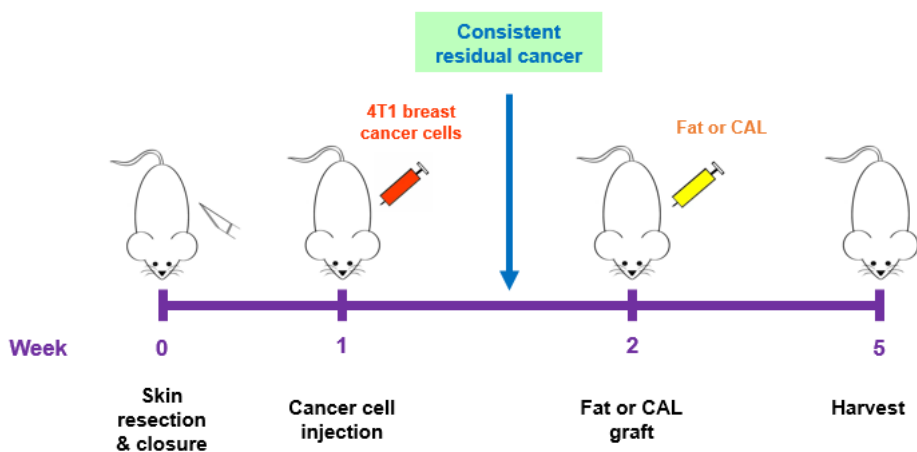


Figure 2. Schematic overview of the animal study design.

To mimic mastectomy (day 0), the mice were administered anesthesia with isoflurane gas and restrained; the skin was sterilized. A 6 mm-long equilateral triangular incision was made, and the superior panniculus carnosus layer was then dissected to

remove the extra skin. On day 7, 4T1 cells suspended in 50  $\mu\text{L}$  phosphate buffered saline were injected into one unique site of the 3rd mammary fat pad where mastectomy was performed. On day 14, the mice were randomized and divided into four experimental groups (n=12, per group, Fig. 2), and CAL was performed in each group as follows: baseline (injection of 100  $\mu\text{L}$  normal saline without fat graft), control (100  $\mu\text{L}$  of fat graft), low CAL ( $2.5 \times 10^5$  ASCs/100  $\mu\text{L}$  fat), and high CAL ( $1 \times 10^6$  ASCs/100  $\mu\text{L}$  fat) groups (Fig. 3). Fat and tumor tissues were harvested for histologic analyses after 3 weeks.

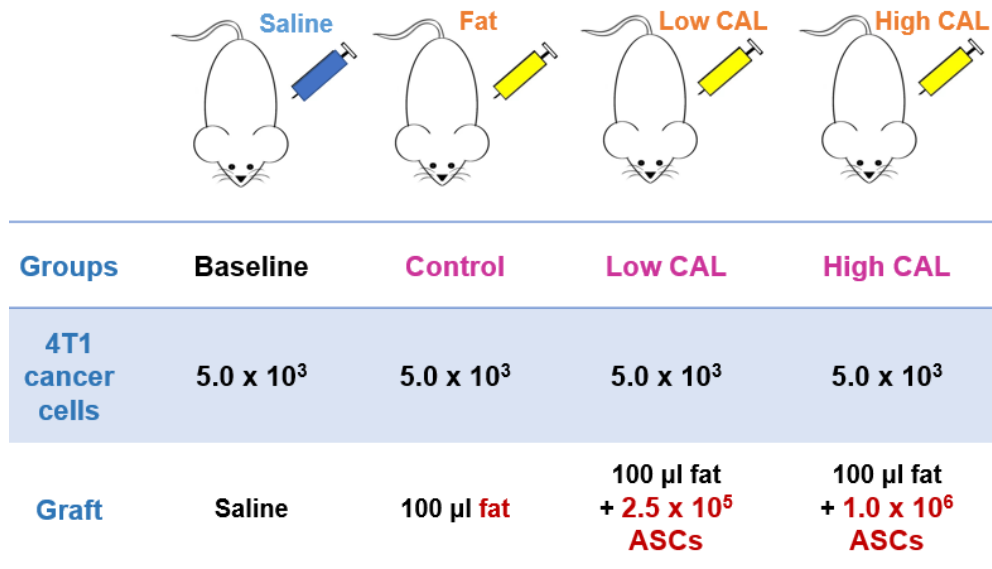


Figure 3. Representative experiment group of baseline, control, low CAL, and high CAL groups injected with 4T1 cells and different concentrations of adipose derived-stromal cells.

### 2.1.3 Histomorphometric evaluation

The isolated fat tumor mass, as well as the liver, lung, and kidney tissues, was fixed with 10% (v/v) neutral buffered formaldehyde

and embedded in paraffin. The samples were sectioned at approximately a 4  $\mu\text{m}$  thickness and stained with H&E [23]. An independent pathologist examined the slides using a light microscope (Nikon ECLIPSE Ts2, Nikon, Tokyo, Japan). The proportional area of the tumor relative to the area of fat tumor mass was measured in every cross-sectional slide using ImageJ software (National Institutes of Health, Bethesda, MD). The ImageJ 'measure stack' plugin was used to calculate the ratio of the tumor in each mass. The weight of the tumor was measured after separated from complex fat tumor mass.

Three embedded tumor samples, randomly selected from each group (n=9), were prepared using a standard protocol [24] and stained for mouse-specific Ki-67 (ab 16667, Abcam Inc, Cambridge, UK) as per the manufacturer's protocol. Ki-67 is a nuclear protein expressed in replicating cells and is often used to calculate the proliferation index in breast cancers [16]. For immunofluorescence staining of grafted fat tissues, the whole-mount staining method was used [25]. First, fat tissues which separated from fat tumor mass were blocked with 5% goat serum (Jackson ImmunoResearch, West Grove, Pa.) in phosphate-buffered saline with 0.03% Triton X-100 for 1 h, incubated overnight at 4° C with either a guinea pig anti-mouse perilipin antibody (20R-PP004; Fitzgerald, Acton, Mass.) or an armenian hamster anti-mouse CD31 antibody (clone 2H8; Merck Millipore, Darmstadt, Germany), and then washed with phosphate-buffered saline with 0.03% Triton X-100. Next, the tissues were incubated with either a goat Cy5-conjugated anti-guinea pig or an Armenian hamster antibody (Jackson ImmunoResearch) for 2 h at room temperature. The tissues were counterstained using DAPI (4',6-

diamidino-2-phenylindole) to visualize the cell nucleus. Immunofluorescence staining images was visualized using a confocal microscope. The vessel area was determined by CD31-positive area per random 0.1-mm<sup>2</sup> region, then measured by the ImageJ software (National Institutes of Health) for the grafted fat vascular density.

#### 2.1.4 Gene expression analysis

Total RNA from grafted fat in three groups was extracted using an RNeasy Lipid Tissue Mini Kit (Qiagen, Hilden, Germany). Reverse transcription was performed using TOPscript<sup>™</sup> RT DryMIX (Enzynomics, Inc., Daejeon, Korea) and quantitative real-time polymerase chain reaction (PCR) was performed using the SYBR Green system (Enzynomics, Inc.). The housekeeping gene (Gapdh) was used as an internal reference. Interleukin-6 (IL-6) was produced as the pro-inflammatory cytokine which was known to modulate the acute immune response to injury. We analyzed the early stage of IL-6 secretion on the postoperative day 7 and the late stage of IL-6 secretion on the postoperative day 21. The grafted fat revascularization level analyzed vascular endothelial growth factor (Vegf) secretion. For sure the ASCs adipogenesis, the peroxisome proliferator-activated receptor  $\gamma$  (Pparg) was analyzed. Primer sequences used in this study are listed in Table 1.

#### 2.1.5 Statistical analysis

Statistical analysis was performed using IBM SPSS version 25 (IBM Corp., Armonk, NY). The Kruskal-Wallis test followed by Dunn's multiple comparison test was used to determine statistical significance between the groups. Data were expressed as the mean



± standard error of the mean, and p-values <0.05 were considered statistically significant.

## 2.2. Results

### 2.2.1 Determining the optimal concentration of 4T1 cells to produce an orthotopic residual breast cancer model

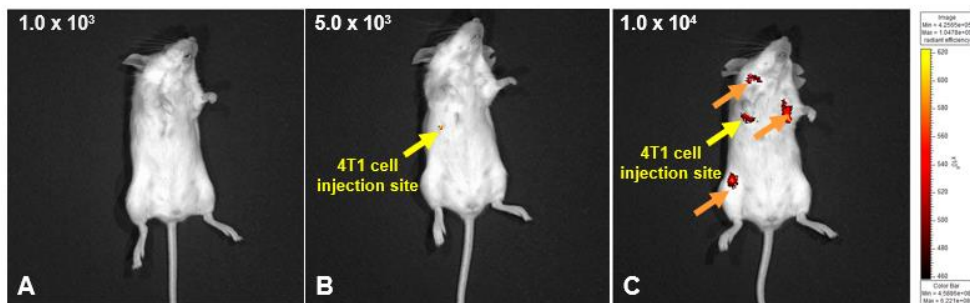


Figure 4. Bioluminescent imaging for determining the optimal number of cancer cells for injection (n=3).

Based on in vivo imaging  $5 \times 10^3$  4T1 cells comprised the most appropriate cell concentration to generate a residual breast cancer model in the 4-week experimental period (Fig. 4A, B, C). Bioluminescent imaging data indicated that the other two concentrations were incompatible with our study, as a tumor mass was not found in the group injected with  $1 \times 10^3$  4T1 cells, whereas tumor metastasis was detected in the group injected with  $1 \times 10^4$  4T1 cells. Therefore, in the following experiment, we inoculated  $5 \times 10^3$  4T1 cells to a mouse 3rd mammary fat pad as the experimental animal model.

## 2.2.2 Quantitative and qualitative analysis of the grafted fat and tumor mass

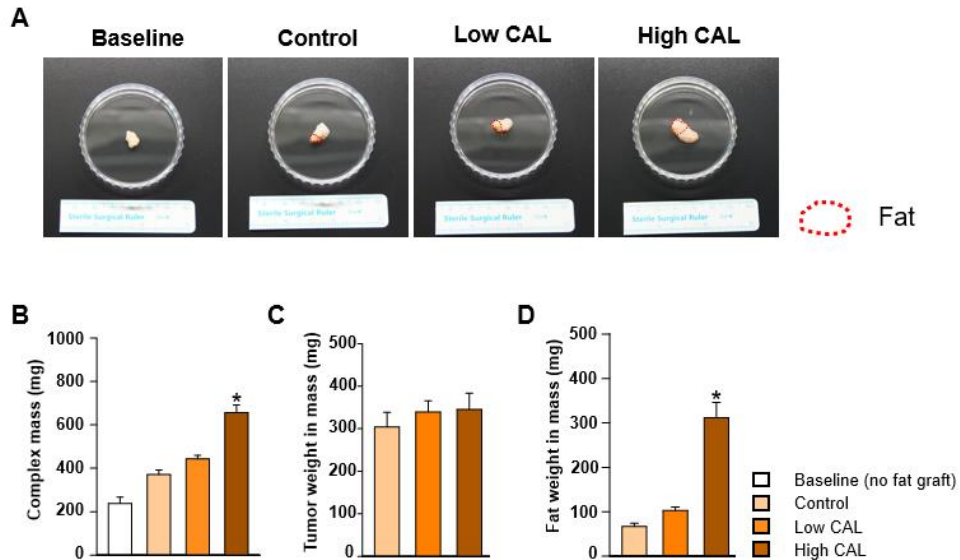


Figure 5. Gross observation and measurement of tumor mass four weeks after injection of 4T1 cells and three weeks after fat/CAL graft (n=12).

Representative fat tumor mass in each group were shown in Fig. 5A and Fig. 6. The weight of the fat tumor mass was significantly higher in the high CAL group than in the baseline group (baseline group: median = 238.0 mg, interquartile range [IQR] = 149–329 mg; high CAL group: median = 655.8 mg, IQR = 589–768 mg;  $p < 0.05$ ,  $n = 12$ ) (Fig. 5B).

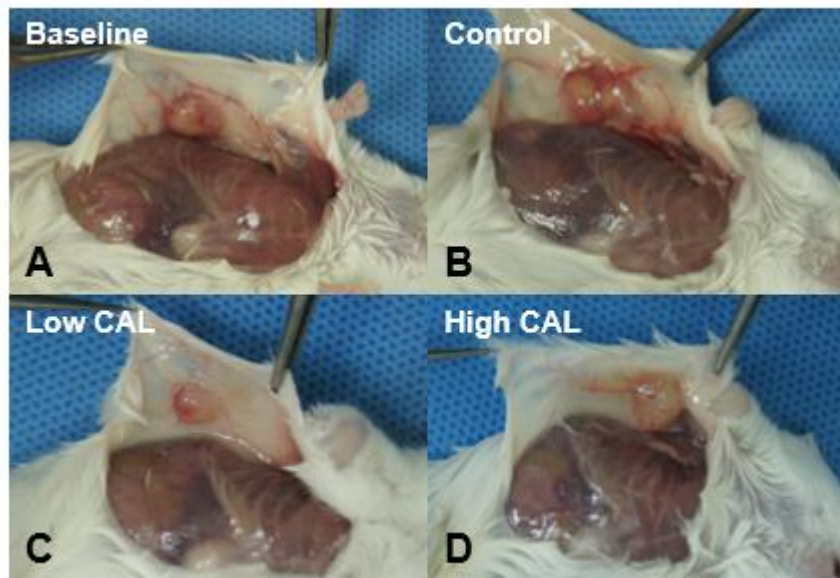


Figure 6. Gross examination of the tumor in the (A) baseline, (B) control, (C) low CAL, (D) and high CAL groups. Images show co-existing tumor and fat graft in the 3rd mammary fat pad, n=12. (Taken with a Canon digital camera 650D, Canon, Tokyo, Japan)

Additionally, the weight in the high CAL group was higher than that in the control and low CAL groups, but this was not statistically significant (control group: median = 370.8 mg, IQR = 317–416 mg; low CAL group: median = 442.6 mg, IQR = 379–471 mg;  $p > 0.05$ , n=12). The tumor weights in the control, low CAL, and high CAL groups were not significantly different (control group: median = 304.2 mg, IQR = 260.1–341.3 mg; low CAL group: median = 339.4 mg, IQR = 290.6–361.1 mg; high CAL group: median = 345.6 mg, IQR = 310.4–404.8 mg;  $p > 0.05$ , n= 12) (Fig. 5C). However, the fat weight was significantly higher in the high CAL group than in the control and low CAL groups (control group:  $66.6 \pm 7.5$  mg; low CAL group:  $103.2 \pm 7.9$  mg; high CAL group:  $310.2 \pm 34.0$  mg;

p<0.05, n= 12) (Fig. 5D). The fat graft survival rate was significantly higher in the high CAL group than in the control and low CAL groups. Concurrently, there was no difference in the change in tumor size among the groups (Fig. 7A).

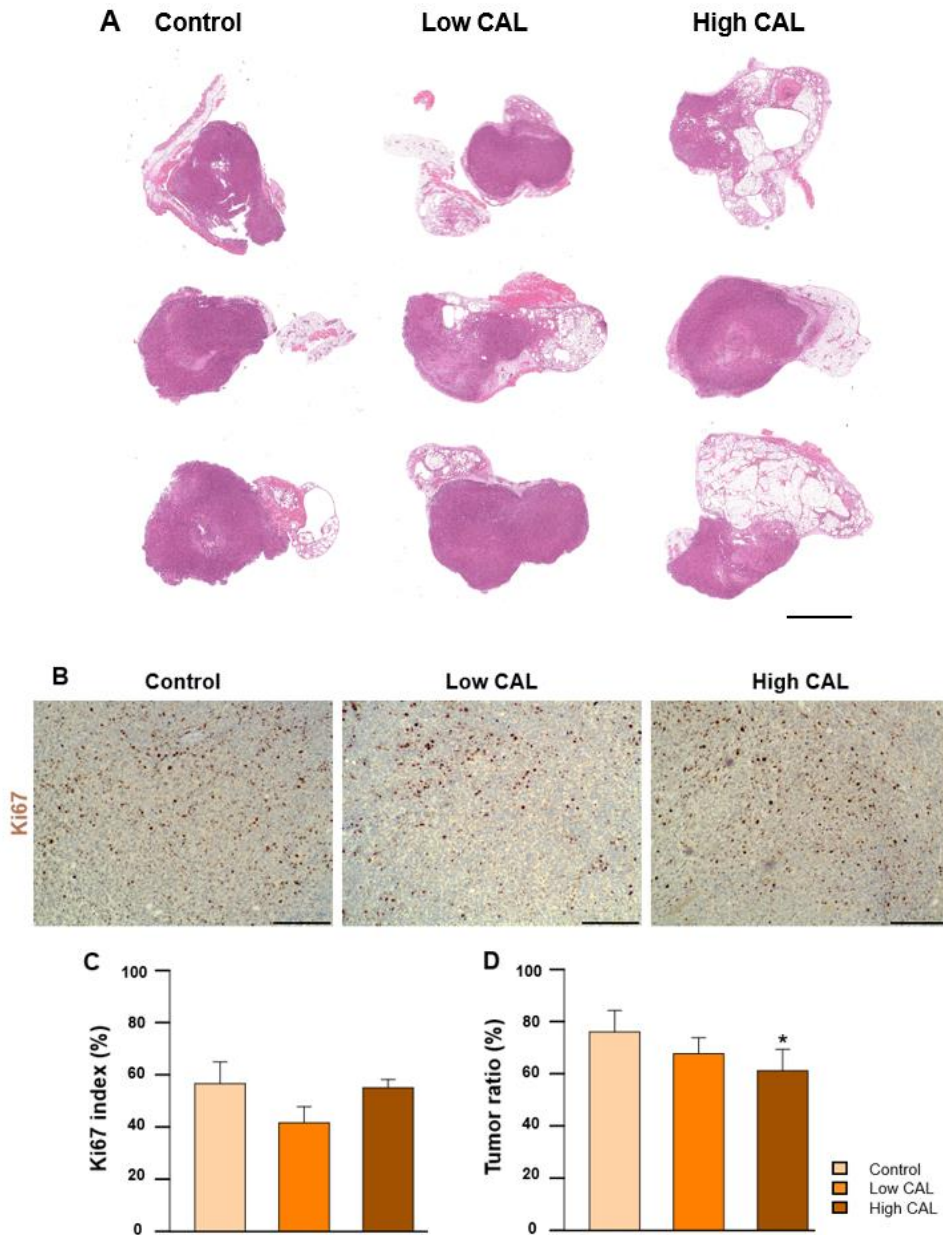


Figure 7. Representative hematoxylin and eosin-stained sections of the fat tumor mass from each group. Measurement of the Ki-67 proliferative index (n= 9).

Based on immunohistochemical analysis of Ki-67 expression to analyze the tumor proliferation rate, no significant difference in the percentage of Ki-67-positive cells was noted among the control, low CAL, and high CAL groups (control group:  $56.67\% \pm 8.26\%$ , IQR = 45-63%; low CAL group:  $41.67\% \pm 6.13\%$ , IQR = 33-46%; high CAL group:  $55.00\% \pm 3.27\%$ , IQR = 51-59%;  $p = 0.0991$ ,  $n = 9$ ) (Fig. 7B, Fig. 7C). The tumor ratio representative that proportional area of the tumor relative to the area of total fat tumor mass. The tumor ratio in high CAL group was significantly lower than control group (control group:  $76.8\% \pm 8.3\%$ , IQR = 73-87%; low CAL group:  $67.7\% \pm 7.6\%$ , IQR = 54-79%; high CAL group:  $61.2\% \pm 8.3\%$ , IQR = 54-72%;  $p = 0.038$ ,  $n = 6$ ) (Fig. 7D). There was no significant difference in tumor size in the three experimental groups in terms of macroscopic view, histological analysis, and weight measurement. Instead, the survival rate of grafted fat was high in the CAL groups. These data indicate that CAL does not change the tumor histological proliferation and portion size change in the cancer residual model, meanwhile CAL could be associated with improved graft fat retention.

2.2.3 CAL enhance grafted fat survival and facilitate the revascularization in grafted fat

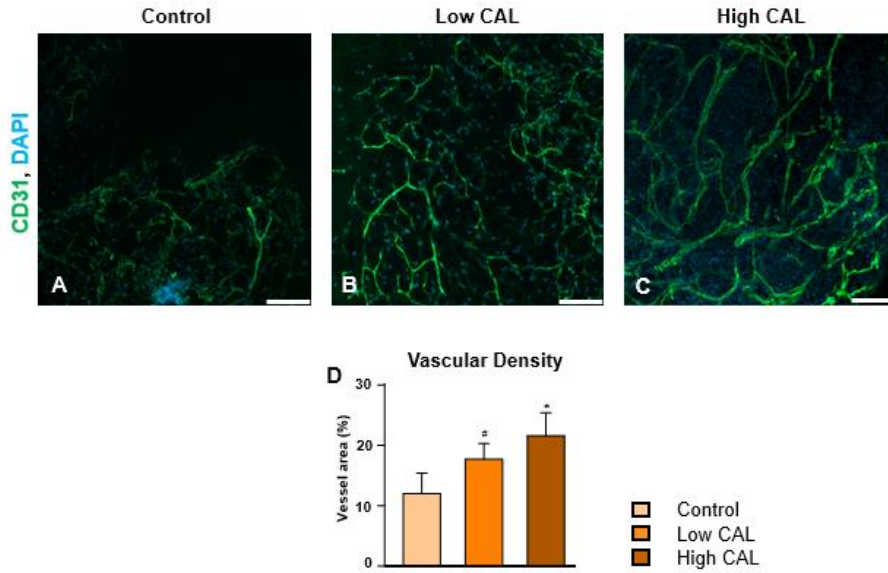


Figure 8. Immunostaining of vessel distribution in grafted fat (n=6).

To investigate the CAL efficacy, we measured the vascular density of the grafted fat by immunofluorescent staining of CD31 (Fig. 8A, B, C). The angiogenesis in grafted fat was considered the factor in the upregulation of fat survival rate. The vascular density of the low CAL group was higher than that of the control group, and the vascular density of the high CAL group was higher than control group (control group: median = 12.12%, IQR = 7.65–15.53%; low CAL group: median = 17.83%, IQR = 13.47–23.45%; high CAL group: median = 22.35%, IQR = 13.63–24.72%;  $p < 0.05$ ; Fig. 8D). Next, according to the confocal imaging results, in the control group, the oil cyst appeared more frequently than in other groups (Fig. 9A, B, C). After the fat graft, adipocytes in the regenerative area survive through graft-derived ASCs adipogenic differentiation [26] known as fat graft replacement theory. And our results indicated that in the high CAL group it was rarely detected ‘dead space’ ,

which showed CAL effectiveness.

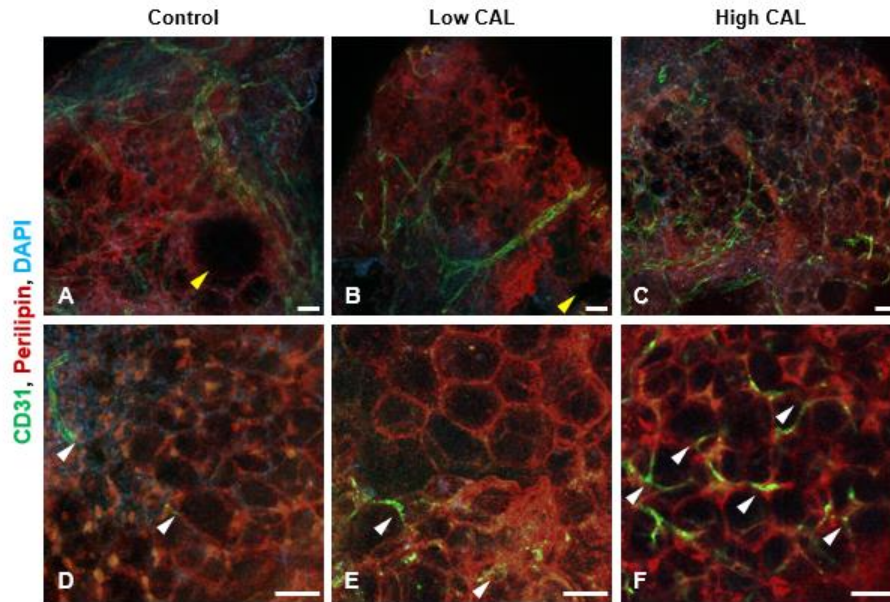


Figure 9. Whole-mount immunostaining of three experimental group grafted fat.

The high magnification confocal image results showed newly regenerated adipocytes in three groups (Fig. 9D, E, F). These data demonstrate that CAL induced increased angiogenesis, the angiogenic effect of ASCs supplemented fat graft can facilitate capillary formation, thereby, increasing revascularization in the grafted fat central portion.

#### 2.2.4 Gene expression analysis

The mRNA expression of different genes from grafted fat and tumor were investigated at postoperative day 7 and day 21 of the experiment. The expression of the IL-6 gene, 7 days after the fat graft and CAL, was significantly higher in the high CAL group compared with the control group (control group: median = 1.06;

high CAL group: median = 1.86;  $p=0.007$ ,  $n = 4$ ). Whereas, 21 days after fat graft and CAL the IL-6 expression levels in the high CAL group were significantly lower than the control group (control group: median = 1.03; high CAL group: median = 0.73;  $p=0.018$ ,  $n = 4$ ) (Fig. 10A). The expression of the Pparg gene, which encodes a key role in adipogenesis and was an essential regulator of adipogenic differentiation, was significantly higher in the high CAL group compared with the control group, meanwhile the low CAL group significantly higher than the control group (control group: median = 0.98 versus low CAL group: median = 2.63,  $p=0.034$ ; control group versus high CAL group: median = 2.81;  $p=0.029$ ,  $n = 4$ ) (Fig. 10B). The expression of the Vegf gene in low CAL group grafted fat and high CAL group grafted fat were significantly higher than in control group grafted fat (control group: median = 1.02 versus low CAL group: median = 3.67,  $p=0.021$ ; control group versus high CAL group: median = 3.04;  $p=0.015$ ,  $n = 4$ ). Whereas the expression of Vegf gene levels in tumors was statistically not different significantly ( $p > 0.05$ ) (Fig. 10C). These findings indicated that CAL could increase the pro-inflammatory effect through IL-6 gene upregulation, however the duration of the effect was mainly in the early period after the fat graft. The upregulation of Vegf gene expression mainly occurs in the grafted fat tissue, indicating that CAL associated revascularization mainly affect grafted fat tissue.



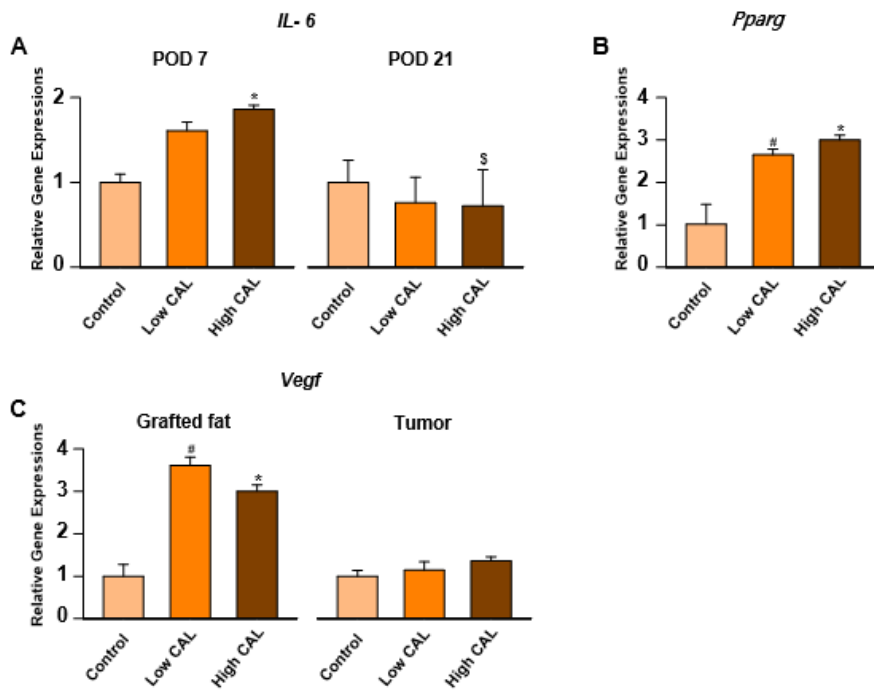


Figure 10. Expression of different genes from grafted fat and tumor

## 2.3. Discussion

The ambiguous role of ASCs in tumor progression has led to safety concerns for clinical therapeutic applications. In addition, in the previous research, information about safety with regards to the concentration of cellular enrichment is lacking. Moreover, an appropriate clinical protocol for ASC-enriched fat grafting has not been established. Given the lack of a standard protocol for ASC-based cell therapy in previous animal studies, the present study focused on the safety of different concentrations of ASCs in CAL and their interaction with residual breast cancer cells.

The ideal animal model for our study to verify the interaction between cancer cells and ASCs in vivo was determined to be a murine cancer model inoculated with human breast cancer cells and human CAL. However, no murine model perfectly mimics human cancer progression [27]; moreover, it is hard to mimic breast cancer recurrence in a murine model. We also highlighted the difficulty in reproducing consistent local recurrence in an animal model; therefore, we decided to use a residual cancer model for the present study. To establish a residual cancer model, both subcutaneous and direct mammary fat pad injection of 4T1 cells were considered. However, the subcutaneous injection of 4T1 cells resulted in the dispersal of cancer cells. Thus, a small incision was made prior to injection, and the 3rd mammary fat pad was targeted as the injection point. Additionally, targeting the 3rd mammary fat pad made it easier to identify and perform fat grafting at the site of tumor cell inoculation (Fig. 11).

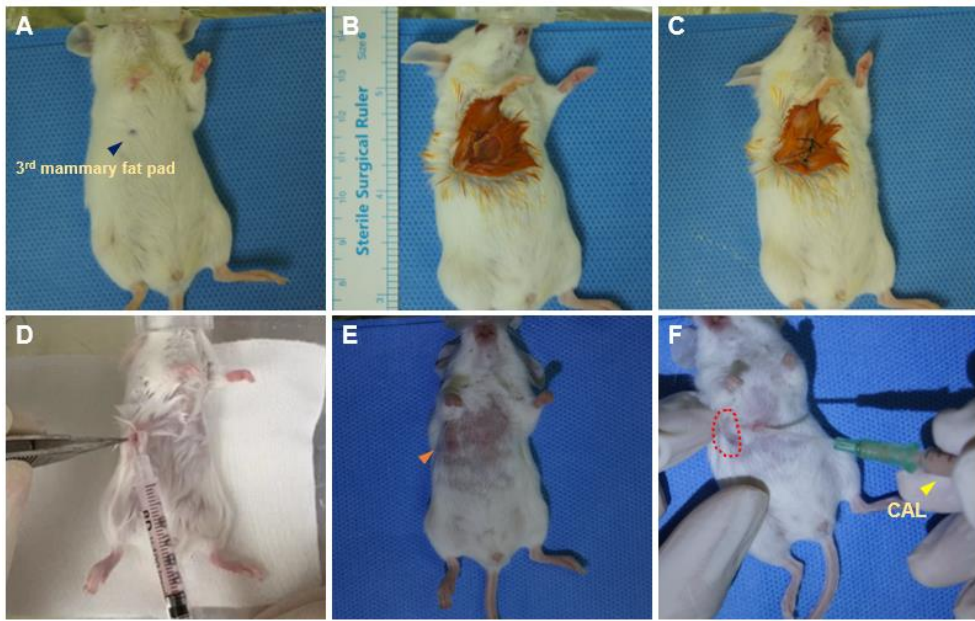


Figure 11. Schematic diagram of animal experiments. (A) The 3rd mammary fat pad was marked using a blue colored pen, (B) and the mastectomy procedure was then performed. (D) Cultured 4T1 cells were counted and directly injected into the 3rd mammary fat pad 7 days after mastectomy. (F) CAL was performed 7 days after injection of 4T1 cells. Using a 1 cc insulin syringe, freshly prepared fat and ASCs were grafted at a site (red dotted point) near the tumor (E; arrow) in the 3rd mammary fat pad.

The grafted fat weight was significantly higher in the high CAL group than in the control and low CAL groups. This suggests that a higher concentration of ASCs improves the fat graft survival rate while maintaining the grafted fat in a better condition; this is consistent with previous studies reporting that higher concentrations of ASCs in enriched fat grafting are associated with increased survival of adipose tissue [28,29]. Similarly, it has also been reported that ASCs exert specific effects when their concentration crosses a threshold value [12].

There was no difference in the Ki-67-positive indexes among the control, low CAL, and high CAL groups, indicating similar tumor proliferation rates. ASCs secrete various cytokines and chemokines [30]. Additionally, it has been reported that some specific paracrine factors in the adipose tissue could exert antitumorigenic effects [31]. Several studies have reported that MSCs can inhibit tumor growth in vivo [10,32,33] and exert potential inhibitory effects on tumor cell growth in vivo without causing host immunosuppression [34]. Additionally, human MSCs have been reported to inhibit breast cancer cell metastasis and growth by inducing apoptosis [35]. Given that ASCs share similar properties with MSCs, they are also thought to exert antitumorigenic effects.

After CAL and fat graft, IL-6 was produced as the pro-inflammatory cytokine which was known to modulate the acute immune response to injury [36]. Our investigations showed that gene expression of IL-6 was upregulated in both low CAL and high CAL groups after 1 week of graft, thus, the early stage of the healing process was more induced in CAL groups. In the previous research [37], IL-6 secreted by ASCs contributed to cell proliferation through activating JAK2/STAT3 pathway and then regulating a proliferation effect on cancer cells. According to our results, in the early stage of the healing process, upregulation of IL-6 was observed in both CAL groups relative to pro-inflammation, whereas at the 3 weeks after fat graft and CAL the IL-6 gene expression in the high CAL group was lower than control group. These results indicated graft fat produced IL-6 mainly effective in the early stage of the healing process.

The grafted fat was in a state of acute ischemia and lack of nutrient supply due to lack of blood supply before revascularization [38,39].

Therefore, revascularization was very important for fat graft survival rate. Meantime, ASCs were well known for promoting revascularization through the secretion of Vegf [40]. And the Vegf plays a key role in angiogenesis. Our results indicate that Vegf expression upregulated in the low CAL and high CAL groups compared with control group. Pparg has been recognized as the master regulator of adipogenesis [41]. Our study confirmed that in CAL groups Pparg relative gene expression was significantly higher than the control group. These results indicated that adipogenesis procedure upregulated in CAL groups. ASCs can directly or indirectly differentiate into endothelial cells [42] and pericytes to promote the formation and stabilization of vascular networks [43, 44] and improve the fat graft survival rate. It is generally believed that the number of ASCs in adipose tissue is closely related to fat transplantation survival [45]. Therefore, the characteristics and concentration of ASCs during fat graft are very important and remain to be solved.

The present study has some limitations. First, the murine breast cancer cell line 4T1 was used in the present study, rather than a human breast cancer cell line. Second, the paracrine effects of ASCs require further investigation since our study focused on animal experiments then measured tumor weight and analyzed Ki-67 index. There is a lack of research on experimental groups that mix 4T1 cells and ASCs in a cellular state and inoculation. Lastly, a residual cancer model was used in the present study owing to difficulties in constructing a local recurrence model. Further research incorporating various concentrations of CAL is needed to evaluate the underlying mechanism.

### 3. Conclusion

In summary, we reported that CAL significantly improves the survival of fat grafts, without significantly affecting the tumor size, in a murine model of residual breast cancer, as demonstrated by the weight of the fat tumor mass and histological analysis. Moreover, higher concentrations of ASCs showed significant efficacy and oncological safety, thus demonstrating the oncologic safety of CAL for breast reconstruction.

## Bibliography

- [1] C. Conrad, R. Huss, Adult stem cell lines in regenerative medicine and reconstructive surgery, *Journal of Surgical Research* 124(2) (2005) 201–208.
- [2] T. Nishimura, H. Hashimoto, I. Nakanishi, M. Furukawa, Microvascular angiogenesis and apoptosis in the survival of free fat grafts, *The Laryngoscope* 110(8) (2000) 1333–1338.
- [3] R. Khouri, D. Del Vecchio, Breast reconstruction and augmentation using pre-expansion and autologous fat transplantation, *Clinics in plastic surgery* 36(2) (2009) 269–280.
- [4] L. Wang, X. Luo, Y. Lu, Z.-H. Fan, X. Hu, Is the resorption of grafted fat reduced in cell-assisted lipotransfer for breast augmentation?, *Annals of plastic surgery* 75(2) (2015) 128–134.
- [5] K.S. Vyas, H.C. Vasconez, S. Morrison, B. Mogni, S. Linton, L. Hockensmith, T. Kabir, E. Zielins, A. Najor, K. Bakri, Fat graft enrichment strategies: a systematic review, *Plastic and reconstructive surgery* 145(3) (2020) 827–841.
- [6] Y. Zhou, J. Wang, H. Li, X. Liang, J. Bae, X. Huang, Q. Li, Efficacy and safety of cell-assisted lipotransfer: a systematic review and meta-analysis, *Plastic and reconstructive surgery* 137(1) (2016) 44e–57e.
- [7] L. Shukla, Y. Yuan, R. Shayan, D.W. Greening, T. Karnezis, Fat therapeutics: the clinical capacity of adipose-derived stem cells and exosomes for human disease and tissue regeneration, *Frontiers in pharmacology* 11 (2020) 158.
- [8] S.F.T. Kølbe, D. Duscher, M. Taudorf, A. Fischer - Nielsen, J.D. Svalgaard, L. Munthe - Fog, B. Jønsson, P.B. Selvig, F.P. Mamsen,

A.J. Katz, Ex vivo - expanded autologous adipose tissue - derived stromal cells ensure enhanced fat graft retention in breast augmentation: A randomized controlled clinical trial, *Stem Cells Translational Medicine* 9(11) (2020) 1277–1286.

[9] F.L. Muehlberg, Y.-H. Song, A. Krohn, S.P. Pinilla, L.H. Droll, X. Leng, M. Seidensticker, J. Ricke, A.M. Altman, E. Devarajan, Tissue-resident stem cells promote breast cancer growth and metastasis, *Carcinogenesis* 30(4) (2009) 589–597.

[10] L. Kucerova, S. Skolekova, M. Matuskova, M. Bohac, Z. Kozovska, Altered features and increased chemosensitivity of human breast cancer cells mediated by adipose tissue-derived mesenchymal stromal cells, *BMC cancer* 13(1) (2013) 1–13.

[11] R. Lin, S. Wang, R.C. Zhao, Exosomes from human adipose-derived mesenchymal stem cells promote migration through Wnt signaling pathway in a breast cancer cell model, *Molecular and cellular biochemistry* 383(1) (2013) 13–20.

[12] K. Li, F. Li, J. Li, H. Wang, X. Zheng, J. Long, W. Guo, W. Tian, Increased survival of human free fat grafts with varying densities of human adipose - derived stem cells and platelet - rich plasma, *Journal of Tissue Engineering and Regenerative Medicine* 11(1) (2017) 209–219.

[13] W. Tsuji, J.E. Valentin, K.G. Marra, A.D. Donnenberg, V.S. Donnenberg, J.P. Rubin, An animal model of local breast cancer recurrence in the setting of autologous fat grafting for breast reconstruction, *Stem cells translational medicine* 7(1) (2018) 125–134.

[14] A.L. Strong, T.A. Strong, L.V. Rhodes, J.A. Semon, X. Zhang, Z. Shi, S. Zhang, J.M. Gimble, M.E. Burow, B.A. Bunnell, Obesity associated alterations in the biology of adipose stem cells mediate



enhanced tumorigenesis by estrogen dependent pathways, *Breast Cancer Research* 15(5) (2013) 1–15.

[15] E.M. Chandler, B.R. Seo, J.P. Califano, R.C.A. Eguluz, J.S. Lee, C.J. Yoon, D.T. Tims, J.X. Wang, L. Cheng, S. Mohanan, Implanted adipose progenitor cells as physicochemical regulators of breast cancer, *Proceedings of the National Academy of Sciences* 109(25) (2012) 9786–9791.

[16] M.M. Silva, M.S. Neto, L.E. Kokai, V.S. Donnenberg, J.L. Fine, K.G. Marra, A.D. Donnenberg, J.P. Rubin, Oncologic safety of fat graft for autologous breast reconstruction in an animal model of residual breast cancer, *Plastic and reconstructive surgery* 143(1) (2019) 103.

[17] K.L. Gale, E.A. Rakha, G. Ball, V.K. Tan, S.J. McCulley, R.D. Macmillan, A case–controlled study of the oncologic safety of fat grafting, *Plastic and reconstructive surgery* 135(5) (2015) 1263–1275.

[18] E. Delay, S. Garson, G. Tousson, R. Sinna, Fat injection to the breast: technique, results, and indications based on 880 procedures over 10 years, *Aesthetic Surgery Journal* 29(5) (2009) 360–376.

[19] D.J. Prockop, M. Brenner, W.E. Fibbe, E. Horwitz, K. Le Blanc, D.G. Phinney, P.J. Simmons, L. Sensebe, A. Keating, Defining the risks of mesenchymal stromal cell therapy, *Cytotherapy* 12(5) (2010) 576–578.

[20] P.A. Zuk, M. Zhu, H. Mizuno, J. Huang, J.W. Futrell, A.J. Katz, P. Benhaim, H.P. Lorenz, M.H. Hedrick, Multilineage cells from human adipose tissue: implications for cell–based therapies, *Tissue engineering* 7(2) (2001) 211–228.

[21] E. Katsuta, M. Oshi, O.M. Rashid, K. Takabe, Generating a murine Orthotopic metastatic breast Cancer model and performing

murine radical mastectomy, *JoVE (Journal of Visualized Experiments)* (141) (2018) e57849.

[22] K.Y. Hong, I.-K. Kim, S.O. Park, U.S. Jin, H. Chang, Systemic administration of adipose-derived stromal cells concurrent with fat grafting, *Plastic and reconstructive surgery* 143(5) (2019) 973e–982e.

[23] H. Chang, S. Hwang, S. Lim, S. Eo, K.W. Minn, K.Y. Hong, Long-term fate of denervated skeletal muscle after microvascular flap transfer, *Annals of plastic surgery* 80(6) (2018) 644–647.

[24] H. Chang, S.O. Park, U.S. Jin, K.Y. Hong, Characterization of two distinct lipomas: a comparative analysis from surgical perspective, *Journal of Plastic Surgery and Hand Surgery* 52(3) (2018) 178–184.

[25] K.Y. Hong, S. Yim, H.J. Kim, U.S. Jin, S. Lim, S. Eo, H. Chang, K.W. Minn, The fate of the adipose-derived stromal cells during angiogenesis and adipogenesis after cell-assisted lipotransfer, *Plastic and Reconstructive Surgery* 141(2) (2018) 365–375.

[26] Y. Yi, W. Hu, C. Zhao, M. Wu, H. Zeng, M. Xiong, W. Lv, Y. Wu, Q. Zhang, Deciphering the emerging roles of adipocytes and adipose-derived stem cells in fat transplantation, *Cell Transplantation* 30 (2021) 0963689721997799.

[27] E. Katsuta, S.C. DeMasi, K.P. Terracina, S. Spiegel, G.Q. Phan, H.D. Bear, K. Takabe, Modified breast cancer model for preclinical immunotherapy studies, *journal of surgical research* 204(2) (2016) 467–474.

[28] F. Lu, J. Li, J. Gao, R. Ogawa, C. Ou, B. Yang, B. Fu, Improvement of the survival of human autologous fat transplantation by using VEGF-transfected adipose-derived stem cells, *Plastic and reconstructive surgery* 124(5) (2009) 1437–1446.

- [29] M. Zhu, Z. Zhou, Y. Chen, R. Schreiber, J.T. Ransom, J.K. Fraser, M.H. Hedrick, K. Pinkernell, H.-C. Kuo, Supplementation of fat grafts with adipose-derived regenerative cells improves long-term graft retention, *Annals of plastic surgery* 64(2) (2010) 222–228.
- [30] G.E. Kilroy, S.J. Foster, X. Wu, J. Ruiz, S. Sherwood, A. Heifetz, J.W. Ludlow, D.M. Stricker, S. Potiny, P. Green, Cytokine profile of human adipose - derived stem cells: Expression of angiogenic, hematopoietic, and pro - inflammatory factors, *Journal of cellular physiology* 212(3) (2007) 702–709.
- [31] R.S. Waterman, S.L. Henkle, A.M. Betancourt, Mesenchymal stem cell 1 (MSC1)-based therapy attenuates tumor growth whereas MSC2-treatment promotes tumor growth and metastasis, (2012).
- [32] L. Kucerova, M. Matuskova, K. Hlubinova, R. Bohovic, L. Feketeova, P. Janega, P. Babal, M. Poturnajova, Bystander cytotoxicity in human medullary thyroid carcinoma cells mediated by fusion yeast cytosine deaminase and 5-fluorocytosine, *Cancer letters* 311(1) (2011) 101–112.
- [33] Y. Zhu, Z. Sun, Q. Han, L. Liao, J. Wang, C. Bian, J. Li, X. Yan, Y. Liu, C. Shao, Human mesenchymal stem cells inhibit cancer cell proliferation by secreting DKK-1, *Leukemia* 23(5) (2009) 925–933.
- [34] Y.-r. Lu, Y. Yuan, X.-j. Wang, L.-l. Wei, Y.-n. Chen, C. Cong, S.-f. Li, D. Long, W.-d. Tan, Y.-q. Mao, The growth inhibitory effect of mesenchymal stem cells on tumor cells in vitro and in vivo, *Cancer biology & therapy* 7(2) (2008) 245–251.
- [35] B. Sun, K.-H. Roh, J.-R. Park, S.-R. Lee, S.-B. Park, J.-W. Jung, S.-K. Kang, Y.-S. Lee, K.-S. Kang, Therapeutic potential of

mesenchymal stromal cells in a mouse breast cancer metastasis model, *Cytotherapy* 11(3) (2009) 289–298.

[36] P.C. Heinrich, I. Behrmann, S. Haan, H.M. Hermanns, G. Müller–Newen, F. Schaper, Principles of interleukin (IL)–6–type cytokine signalling and its regulation, *Biochemical journal* 374(1) (2003) 1–20.

[37] H.–J. Wei, R. Zeng, J.–H. Lu, W.–F.T. Lai, W.–H. Chen, H.–Y. Liu, Y.–T. Chang, W.–P. Deng, Adipose–derived stem cells promote tumor initiation and accelerate tumor growth by interleukin–6 production, *Oncotarget* 6(10) (2015) 7713.

[38] Y. Chen, Y. Chai, B. Yin, X. Zhang, X. Han, L. Cai, N. Yin, F. Li, Washing Lipoaspirate Improves Fat Graft Survival in Nude Mice, *Aesthetic Plastic Surgery* (2022) 1–14.

[39] H. Kato, K. Mineda, H. Eto, K. Doi, S. Kuno, K. Kinoshita, K. Kanayama, K. Yoshimura, Degeneration, regeneration, and cicatrization after fat grafting: dynamic total tissue remodeling during the first 3 months, *Plastic and reconstructive surgery* 133(3) (2014) 303e–313e.

[40] J. Yang, Y. Zhang, G. Zang, T. Wang, Z. Yu, S. Wang, Z. Tang, J. Liu, Adipose - derived stem cells improve erectile function partially through the secretion of IGF - 1, bFGF, and VEGF in aged rats, *Andrology* 6(3) (2018) 498–509.

[41] J. Stachecka, J. Nowacka–Woszek, P.A. Kolodziejcki, I. Szczerbal, The importance of the nuclear positioning of the PPARG gene for its expression during porcine in vitro adipogenesis, *Chromosome Research* 27(3) (2019) 271–284.

[42] T. Tsuchiya, N. Mitsutake, S. Nishimura, M. Matsuu–Matsuyama, Y. Nakazawa, T. Ogi, S. Akita, H. Yukawa, Y. Baba, N. Yamasaki, Transplantation of bioengineered rat lungs recellularized

with endothelial and adipose-derived stromal cells, *Scientific reports* 7(1) (2017) 1–15.

[43] N.F. Gontijo-de-Amorim, L. Charles-de-Sá, G. Rigotti, Fat grafting for facial contouring using mechanically stromal vascular fraction-enriched lipotransfer, *Clinics in Plastic Surgery* 47(1) (2020) 99–109.

[44] N. Simonavicius, M. Ashenden, A. Van Weverwijk, S. Lax, D.L. Huso, C.D. Buckley, I.J. Huijbers, H. Yarwood, C.M. Isacke, Pericytes promote selective vessel regression to regulate vascular patterning, *Blood, The Journal of the American Society of Hematology* 120(7) (2012) 1516–1527.

[45] K.J. Paik, E.R. Zielins, D.A. Atashroo, Z.N. Maan, D. Duscher, A. Luan, G.G. Walmsley, A. Momeni, S. Vistnes, G.C. Gurtner, Studies in fat grafting: part V. Cell-assisted lipotransfer to enhance fat graft retention is dose dependent, *Plastic and reconstructive surgery* 136(1) (2015) 67.

## Table

Table 1. Primer sequences for quantitative real-time polymerase chain reaction

Gene	Sequence	
<i>IL-6</i>	Forward	5' – ATAGTCCTTCCTACCCCAATTTCC – 3'
	Reverse	5' – GATGAATTGGATGGTCTTGGTCC – 3'
<i>Vegf</i>	Forward	5' – CATCTTCAAGCCGTCCTGTGT – 3'
	Reverse	5' – CACTCCAGGGCTTCATCGTTA – 3'
<i>Pparg</i>	Forward	5' – TGCACTGCCTATGAGCACTTCA CA – 3'
	Reverse	5' – AGGAATGCGAGTGGTCTTCCAT CA – 3'
<i>Gapdh</i>	Forward	5' – GGCCCGGTGCTGAGTATGTC – 3'
	Reverse	5' – TGCCTGCTTCACCACCTTCT – 3'

## Figure Legends

Figure 1. Schematic figure of the cell-assisted lipotransfer (CAL). Harvested fat was divided into two parts, SVF cells are obtained through the isolation method. After harvesting enough SVF or ASCs, mix with the remaining fat to obtain ASC-rich fat.

Figure 2. Schematic overview of the animal study design. First, skin resection and closure were performed to mimic mastectomy. After one week, 4T1 cells were injected into the 3rd mammary fat pad of mice. Two weeks after mastectomy, fat grafting was performed. Four weeks after 4T1 cells injection and three weeks after fat grafting, the mice were sacrificed. Abbreviations: CAL, cell-assisted-lipotransfer.

Figure 3. Representative experiment group of baseline, control, low CAL, and high CAL groups injected with 4T1 cells and different concentrations of adipose derived-stromal cells.

Figure 4. Bioluminescent imaging for determining the optimal number of cancer cells for injection.

Representative bioluminescence images of mice injected with different concentrations of GFP-expressing 4T1 cells, (A)  $1 \times 10^3/50 \mu\text{L}$ , (B)  $5 \times 10^3/50 \mu\text{L}$ , (C) and  $1 \times 10^4/50 \mu\text{L}$ , taken 4 weeks after injection. The group injected with  $1 \times 10^3$  GFP-expressing 4T1 cells showed poor tumor formation. The group injected with  $5 \times 10^3$  GFP-expressing 4T1 cells had a localized tumor in the 3rd mammary fat pad (injection site; yellow arrow)

without dramatic metastasis. The group injected with  $1 \times 10^4$  GFP-expressing 4T1 cells showed metastasis to multiple sites (orange arrow).

Figure 5. Gross observation and measurement of tumor mass four weeks after injection of 4T1 cells and three weeks after fat/CAL graft.

(A) Macroscopic view of the fat tumor mass in the baseline, control group, low CAL, and high CAL groups. (B) Graph summarizing the weight of the fat tumor mass in each group. \* $p < 0.05$  versus control and high CAL groups. (C) Tumor weight among three experiment groups was not statistically significant. (D) Fat weight was histologically evaluated. The fat graft survival rate was the highest in the high CAL group. \* $p < 0.05$  versus control and high CAL groups. Grafted fat is outlined by a red dotted circle. Error bars = standard error of mean (SEM). Abbreviations: low CAL, low concentration adipose-derived stromal cell cell-assisted lipotransfer; high CAL, high concentration adipose-derived stromal cell cell-assisted lipotransfer.

Figure 6. Gross examination of the tumor in the (A) baseline, (B) control, (C) low CAL, (D) and high CAL groups. Images show co-existing tumor and fat graft in the 3rd mammary fat pad (right; taken with a Canon digital camera 650D, Canon, Tokyo, Japan)

Figure 7. Representative hematoxylin and eosin-stained sections of the fat tumor mass from each group. Measurement of the Ki-67 proliferative index.

(A) The grafted fat survival rate and fat density were the highest in



the high CAL group. Survived fat graft is outlined by a red dotted circle. Grafted fat is outlined by a black dotted circle. Scale bar = 3 mm. Abbreviations: low CAL, low concentration adipose-derived stromal cell cell-assisted lipotransfer; high CAL, high concentration adipose-derived stromal cell cell-assisted lipotransfer. (B) Immunohistochemical analysis for Ki-67 expression in a representative tumor from the control, low CAL and high CAL groups. (C) Percentage of Ki-67-positive cells in the low CAL and high CAL groups. The proliferation index is indirectly representative of the tumor-ASC interaction. (D) The tumor ratio in high CAL group was significantly lower than control group, the proportion measured by cross-section image of hematoxylin and eosin-stained slides. \* $p < 0.05$  versus control and high CAL groups. Error bars = SEM Scale bars = 200  $\mu\text{m}$

Figure 8. Immunostaining of vessel distribution in grafted fat.

(A, B, C) Immunofluorescent staining of grafted fat after sacrifice. (D) Vascular density of the grafted fat measured by quantification of CD31 immunofluorescent staining at postoperative week 3. The vascular density of the high CAL group is higher than that of the control group, and the vascular density of the low CAL is higher than that of the control group. \* $p < 0.05$  versus the control group. # $p < 0.05$  versus the control group. Scale bars = 50  $\mu\text{m}$ .

Figure 9. Whole-mount immunostaining of three experimental group grafted fat.

Immunofluorescent staining of grafted fat in control group (A), low CAL (B), and high CAL groups (C). High magnification confocal image of grafted fat in control group (D), low CAL (E), and high

CAL group (F). The yellow arrows indicate oil cyst occurred in grafted fat. The white arrows indicate capillary appearance under the high magnification view. The tissues were counterstained using DAPI to visualize the cell nucleus. Scale bars = 50  $\mu$ m.

Figure 10. Expression of different genes from grafted fat and tumor. Gene expression analyses of IL-6 (A), Pparg (B) and Vegf (C) by quantitative real-time polymerase chain reaction. Data are expressed as fold-changes in relation to levels in the control group. Statistically significant differences among groups are reported above the columns. #p < 0.05 control group versus the low CAL group. \*p < 0.05 control group versus the high CAL group. \$p < 0.05 control group versus the high CAL group.

Figure 11. Schematic diagram of animal experiments. (A) The 3rd mammary fat pad was marked using a blue colored pen, (B) and the mastectomy procedure was then performed. (D) Cultured 4T1 cells were counted and directly injected into the 3rd mammary fat pad 7 days after mastectomy. (F) CAL was performed 7 days after injection of 4T1 cells. Using a 1 cc insulin syringe, freshly prepared fat and ASCs were grafted at a site (red dotted point) near the tumor (E; arrow) in the 3rd mammary fat pad.

## 국문초록

### 유방암 잔여 동물모델에서 지방재건을 위한 세포 보조 지방이식의 종양학적 안전성 및 유효성

**서론:** 세포 보조 지방이식(CAL)은 자가 지방과 지방 유래 기질 세포(ASCs)를 함께 이식하여 지방 생착을 향상시키는 새로운 지방 이식 술기입니다. 그러나 지방 유래 기질 세포의 사용으로 인하여 종양학적 안전성 측면에서 논란이 있습니다.

**방법:** 유방 재건을 위한 CAL의 종양학적 안전성을 연구하기 위하여 설치류 유방암 잔여 동물모델을 제작하였습니다. 다양한 농도의 4T1 세포(설치류 유방암 세포)를 유방 절제된 암컷 BALB/c 마우스의 3<sup>rd</sup> 유선 부위에 주사하여 동물모델로 적합한 농도 ( $5.0 \times 10^3$  4T1)를 결정하였습니다. 주사 1주일 후, 마우스를 대조군( $100 \mu\text{L}$  지방), 저농도 CAL( $2.5 \times 10^5$  ASCs/ $100 \mu\text{L}$  지방) 및 고농도 CAL( $1.0 \times 10^6$  ASCs/ $100 \mu\text{L}$  지방) 그룹으로 나누어 지방 이식을 수행했습니다.

**결과:** 이식된 지방조직과 생성된 종양조직의 복합조직을 분석한 결과, 그 무게는 고농도 CAL 그룹에서 다른 그룹에서보다 유의하게 더 높았습니다 ( $p < 0.05$ ). 그러나 계측된 종양부분의 무게는 그룹 간에 유의미한 차이가 없었습니다. 또한, 지방이식 생존율은 대조군과 저농도 CAL 군보다 고농도 CAL 군에서 유의하게 더 높았습니다 ( $p < 0.05$ ). Ki-67 양성 세포의 비율에는 유의한 차이가 나타나지 않았으며, 따라서 종양 증식이 그룹 간에 유의한 차이가 없음을 알 수 있습니다.

**결론:** CAL은 유방암 잔여 동물에서 종양 크기와 증식에 영향을 미치지 않으면서 이식된 지방의 생존을 유의하게 개선했습니다. 따라서, 유방 재건을 위한 세포 보조 지방이식은 관찰 시간 내에서 그 효과의 유효성과 종양학적 안전성을 가집니다.

---

주요어: 지방유래 줄기세포, 세포 보조 지방이식, 지방이식, 지방재건,  
설치류 지방암 동물모델

학번: 2020-36902